RESEARCH ARTICLE

Selenium Nanoparticle Enhanced Photodynamic Therapy against Biofilm forming *Streptococcus mutans*

Zarrin Haris[1]*, Asad U Khan[2]

[1]Research scholar, Interdisciplinary Biotechnology Unit, Aligarh Muslim University, Aligarh, India

[2]Professor, Interdisciplinary Biotechnology Unit, Aligarh Muslim University, Aligarh, India

[*]***Address for Correspondence: Ms. Zarrin Haris, Research scholar, Interdisciplinary Biotechnology Unit, Aligarh Muslim University, Aligarh, India***

Received: 25 June 2017/Revised: 23 July 2017/Accepted: 27 August 2017

ABSTRACT- Present work explores the novel selenium nanoparticle-enhanced photodynamic therapy of toluidine blue O against *Streptococcus mutans* biofilm. Physiochemical (Ultraviolet-visible absorption, FTIR, and fluorescence spectroscopy) and Electron microscopy techniques were used to characterize selenium nanoparticles. The UV spectrum of different concentrations of SeNP were showed distinct peak at ~288 nm, which confirmed the successful synthesis of SeNP in this study. The synthesized Selenium nanoparticles were uniform and spherical in shape with average size ~100 nm. In FTIR spectra of SeNPs there were strong absorption band around 3425cm^{-1}, 2928 cm^{-1} and 1647 cm^{-1}. TBO showed MIC and MBC of 62.5 µg/mL and 125 µg/mL respectively whereas in presence of SeNPs showed MIC and MBC of 31.25 µg/mL and MBC of 62.5 µg/mL. SeNPs–TBO conjugate showed twofold higher activities against *S mutans* than TBO alone. A 630 nm diode laser was applied for activation of SeNP- Toluidine blue O (TBO) combination and TBO against *S. mutans* biofilm and cells. The UV-vis absorption result suggests that TBO is not present on the surface of SeNP. In fluorescence emission spectra, there is enhancement of fluorescence of TBO fluorescence in the presence of nanoparticle. This showed that SeNP are enhancing the photodynamic therapy. Antibiofilm assays and microscopic studies showed significant reduction of biofilm presence of conjugate. A crystal violet assay revealed a maximum percent inhibition of *S. mutans* biofilm formation after 24 hours' incubation, recorded as 20% and 60% by TBO (31.25 µg/mL) and SeNP–TBO (31.25 µg/mL; TBO) conjugate, respectively. XTT biofilm reduction assay were showed 32% loss in viability in presence of SeNP-TBO conjugate whereas in presence of only TBO there was 22% loss in viability of cells. Fluorescence spectroscopic study confirmed type I photo toxicity against biofilm. Selenium nanoparticle conjugate–mediated photodynamic therapy may be used against recalcitrant biofilm based infections and can be helpful in dentistry.

Key-words- *S. mutans*, SeNP, TBO, UV absorption, FTIR, fluorescence spectroscopy

INTRODUCTION

Microorganisms have traditionally been considered as planktonic, freely suspended cells. However in their natural environment bacteria forms biofilm communities which are sessile organisms embedded in hydrated extracellular polymeric matrix. [1]

Biofilms are spatially structured heteromorphic microbial communities ensconced in exopolymeric matrix material.[2-3] It has been shown that a substantial amount of microbial infections occur through biofilm formation.[4] The formation of biofilm is a dynamic process. In process of biofilm formation the bacteria undergo a coordinated series of molecular events in response to the environmental signals that leads to the expression of new phenotypes. [5-6] In addition to responses to physical and chemical signals, bacteria regulate diverse physiological processes in a cell density-dependent manner, commonly called quorum sensing. Bacteria constantly secrete low levels of these signals and sense them through the corresponding receptors.[7] The receptors do not trigger any behavioral changes until there are enough bacteria to allow the signal concentrations to exceed a critical threshold. [8-9] Once this occurs, bacteria respond by adopting communal behaviour, such as forming biofilms.

Biofilm are inherently resistant to both antimicrobial agents and host defenses and therefore are the root cause of many persistent bacterial infections. [10] Biofilm is highly resistant against drug molecules as compared to planktonic cells. [11] Dental plaque is one of the best-studied biofilms. *Streptococcus mutans* has been proven to be one of the prime offenders in cariogenesis. [12]

The term virulence defines the ability of a particular microbe to cause infectivity. This property is quantitative

Access this article online	
Quick Response Code	Website: www.ijlssr.com
	DOI: 10.21276/ijlssr.2017.3.5.4

and expresses the degree of pathogenicity. The virulence factors of microbe helps it to protect or defend itself against the host and maintain its favourable environment, same occurs in case of *S. mutans*, it has various virulence factors that helps its anchoring the tooth surface in case of dental carries, and contributes to its ability to cause host damage. Adhesins, Glucosyl transferases and fructosyl transferases, Acidogenicity and Acid Tolerance are the virulence factors. Treatment techniques involve either periodic mechanical disruption of oral microbial biofilms or maintaining therapeutic concentrations of antimicrobials in the oral cavity, both of which are fraught with limitations. The development of alternative antibacterial therapeutic strategies therefore becomes important in the evolution of methods to control microbial growth in the oral cavity. The use of photodynamic therapy for inactivating microorganisms was first demonstrated more than 100 years ago, when Oscar Raab reported the lethal effect of acridine hydrochloride and visible light on *Paramecia caudatum*. Photodynamic therapy for human infections is based on the concept that an agent (a photosensitizer) which absorbs light can be preferentially taken up by bacteria and subsequently activated by light of appropriate wavelength in the presence of oxygen to generate singlet oxygen and free radicals that are cytotoxic to microorganisms. Because of the primitive molecular nature of singlet oxygen, it is unlikely that microorganisms would develop resistance to the cytotoxic action. Photodynamic therapy has emerged as an alternative to antimicrobial regimes and mechanical means in eliminating dental plaque species as a result of the pioneering work of Prof. Michael Wilson and colleagues at the Eastman Dental Institute, University College London, UK. Photodynamic therapy (PDT) is a treatment modality for several diseases, most notably cancer. PDT involves three separate components: a photosensitizer (PS), light activation and molecular oxygen. The combination of these components produces reactive oxygen species (ROS) and leads to the destruction of target cells. There are two classes of ROS, one created through electron transfer (Type I reaction) and the other by energy transfer (Type II reaction). Electron transfer to O_2 can produce superoxide, hydrogen peroxide and hydroxyl radicals. In a Type II reaction, energy transfer to O_2 results in the formation of singlet oxygen ($^1O_2$).[13] Both Type I and Type II photochemical reactions depend on several parameters, most importantly, the photosensitizer used and the concentration of oxygen. [14] Oxygen in its excited singlet state ($^1O_2$) is likely the most important intermediate in these reactions. [15-16] It is one of several ROS that can induce antioxidative processes and deteriorate biological tissues, damage essential cell components, such as the cytoplasmic membrane, or irreversibly alter metabolic activities, resulting in cell death. [17-19] Incomplete penetration of photoactive compound in oral biofilm may become greater in a clinical setting, where both the photoactive compound and light should be applied for periods of up to several min. Therefore, one of the ways to overcome these deficiencies is to develop delivery systems that significantly improve the pharmacological characteristics of photoactive compound. Nanoparticle have been successfully included in PDT to improve the therapy of cancer, through a combination of enhanced drug delivery and light absorption.[20] Furthermore nanoparticles have been prepared for diagnostic assay based on PDT.[21] There is a vast literature concerning the application of nanoparticle in cancer treatment but little have been done on the antimicrobial aspects of such interactions. The drive in the development of non antibiotic based approaches for treating infectious diseases have been instrumental in expanding the application of antimicrobial techniques such as PDT. The increasing isolation of bacterial species showing resistance to antibiotics is a growing concern of health authorities around the world: grand efforts have been dedicated to improvement of performance antimicrobial PDT through the design of new Photosensitizer or using nanoparticles.

In present study we have used Selenium nanoparticle enhanced photodynamic therapy against *S. mutans* biofilm. It is a new combination for enhancement of performance of antimicrobial photodynamic therapy processes in coupling nanotechnology to PDT.

MATERIALS AND METHODS

Bacterial Cultures and Growth Conditions

The *Streptococcus mutans* MTCC 497 (Institute of Microbial Technology, Chandigarh, India), bacterial strain used in this study, was obtained from the culture stocks of our laboratory, Interdisciplinary Biotechnology Unit, AMU Aligarh, subcultured in Brain Heart Infusion (BHI) Broth (Himedia Labs, Mumbai, India) supplemented with 5% sucrose, at 37ºC, which is known to induce robust biofilm formation.

Synthesis of Selenium Nanoparticles by chemical reduction method

Selenium nanoparticles were synthesized in colloidal form by chemical reduction method. [22] First 100m M ascorbic acid was added into 25m M sodium seleniate under magnetic stirring and it was reconstituted to a final volume with milli-q water. Gradually the color of solution changes from transparent to orange, indicating colloidal SeNPs formation.

Characterization Methods of Synthesized Selenium Nanoparticles (SeNP)

Selenium nanoparticles were further characterized by UV-Visible spectroscopy, transmission electron microscopy, and FT-IR (Fourier transform infra-red) spectroscopy briefly described as follows.

The synthesis of selenium nanoparticle in solution was monitored by measuring the absorbance (A) using UV-Vis spectrophotometer in the wavelength range of 200 to 800 nm. The vacuum dried selenium nanoparticle powder was stored in amber colour vials at room temperature under dry and dark condition form until used for further characterization.

Transmission electron microscopy (TEM) was used to determine the actual size, shape, and pattern of arrangement of synthesized SeNP. Colloidal SeNP droplets were placed on a copper grid and dried in desiccators before viewing under a field-emission electron microscope (JEM-2100F; Jeol, Tokyo, Japan) at 120 kV voltage.

FTIR measurement SeNP was carried out with a Nicolet Magna 750 FT-IR spectrophotometer (DTGS detector, Ni-chrome source and KBr beam splitter; Thermo Fisher Scientific, Waltham, MA) with a total of 100 scans and resolution of 16 cm^{-1} at a range of 400–4000 cm^{-1}, using silver bromide windows at room temperature.

Photosensitization of TBO and SeNP–TBO Conjugate

Toluidine blue O (TBO) was used as a photosensitizer. A stock solution of 1 mmol L^{-1} TBO (Sigma-Aldrich, St Louis, MO, USA) was prepared in DW. This solution was filtered-sterilized, and stored at -20^{0}C in the dark. Working solutions were obtained by diluting the stock solutions with PBS to 20 µmol L^{-1}.

TBO and SeNP–TBO conjugate were activated or photosensitized during treatment against *S. mutans* biofilm and *S. mutans* cells. Laser (ML101J27; Mitsubishi, Tokyo, Japan) with 630-nm wavelength light source and output power of 120 mW was used for photosensitization. A laser illuminated area of 0.12 cm^2 with energy density of 38.2 J/cm^2 was used for 60 seconds for both TBO and conjugate activation. In all *S. mutans* antibiofilm and antimicrobial assays, TBO and SeNP-TBO conjugate were treated and activated at 6 and 18 hours during 12 and 24-hour incubation periods respectively.

Spectroscopic Measurements of SeNP-TBO Conjugate

A double-beam UV-visible spectrophotometer (Perkin Elmer) was used to characterize the synthesized SeNP and measure the mode of interaction of SeNP with TBO photosensitizer. Scanning was in the 200–800 nm wavelength range.

Fluorescence spectra were recorded on a Hitachi (Tokyo, Japan) F-4500X fluorescence spectrometer controlled by a personal computer data-processing unit. The excitation was done at 595 nm and the emission spectra from 610 nm to 800 nm were collected. All excitation and emission slits were set at 1.5 nm.

Determination of Minimum inhibitory concentration (MIC) and Minimum Bactericidal Concentration (MBC)

Minimum inhibitory concentration (MIC) was determined by broth dilution method as recommended by CLSI guidelines, in which two fold serial dilution of the TBO (initial concentration1.0mg/mL) was performed and 50µl of SeNP was added in each well. The MIC was determined as the lowest concentration that totally inhibits visible bacterial growth. Minimum bactericidal concentration (MBC) of TBO and TBO-SeNP conjugate was determined by sub culturing the test dilutions on to a fresh solid medium and incubated for 24 hours.

Biofilm Reduction (Crystal Violet Staining Assay)

Biofilms were produced on commercially available presterilized, polystyrene, flat-bottom 96-well microtiter plates. Control, SeNP, TBO, and SeNP–TBO conjugate-treated *S. mutans* biofilm were assessed by microdilution method and quantified by crystal violet (HiMedia) assay [23-24]. Treated and control biofilm-coated wells of microtiter plates were washed twice with 200 µL of PBS and then air-dried for 45 minutes. Then, each of the washed wells was stained with 110 µL of 0.4% aqueous crystal violet solution for 45 minutes. Afterwards, each well was washed four times with 350 µL of sterile distilled water and immediately de-stained with 200 µL of 95% ethanol. After 45 minutes of de-staining, 100 µL of de-staining solution was transferred to a new well and the amount of the crystal violet stain in the de-staining solution measured with a microtiter plate reader (iMark; Bio-Rad, Hercules, California) at 595 nm. The absorbance for the controls was subtracted from the test values to minimize background interference.

XTT Biofilm Reduction Assay

In this assay 2,3-Bis (2-methoxy-4-nitro-5-sulfophenyl)-5-([phenylamino] carbonyl)-2H-tetrazolium hydroxide (XTT) (Sigma-Aldrich) was dissolved in PBS at a final concentration of 1 mg/L. The solution was filter sterilized using a 0.22-mm pore-size filter and stored at −70°C until required. Menadione (Sigma-Aldrich) solution (0.4 mM) was also prepared and filtered immediately before each assay. Prior to each assay, XTT solution was thawed and mixed with menadione solution at a volume ratio of 20:1. The adherent cells in treated and control *S. mutans* biofilm, as previously described in crystal violet assay, were washed four times with 200 µL of PBS to remove loosely adherent or planktonic cells. Afterwards, 158 µL of PBS, 40 µL of XTT, and 2 µL of menadione inoculated each of the prewashed wells. After incubation in the dark for 4 hours at 37°C, 100 µL of the solution was transferred to a new well and a colorimetric change in the solution measured using a microtiter plate reader (iMark) at 490 nm [25].

Microscopic Studies of Reduction of Biofilm

To analyse the effect of the crude extracts on biofilm, cells were grown on saliva-coated glass coverslips. *Streptococcus mutans* was grown in BHI supplemented with 5% sucrose in a botton glass cover dishes. The experiment was done in triplicates. Sub- MIC concentration of the SeNP and TBO was taken while the control was untreated. The plates were inoculated and incubated at 37ºC for 24 h. The media was removed from plates and washed with sterile PBS to remove the unattached cells. It was then stained with propidium iodide for 1 h. Fluorescence emission was observed using Fluorescence microscope (Fluoview FV200). The excitation wavelength was 594 nm [26].

Measurement of Reactive Oxygen Species (ROS) Production

Amount of ROS was measured by fluorometric assay, done with DCFH-DA [27]. Briefly, the cells were adjusted to an OD 600 of 1 in 10 ml of PBS and centrifuged at 5000x g for 10 min. The cell pellet was then resuspended in PBS and treated with SeNP, TBO and TBO-SeNP conjugate (31.25µg/ml). After incubation with SeNP, TBO and TBO-SeNP conjugate at 37°C for different time intervals (0-60 min), 10 µM 2,7-dichlorofluorescein diacetate (DCFH-DA) in PBS was added. The fluorescence intensities (excitation 485 nm and emission 540 nm respectively) of the resuspended cells were measured with a spectrofluorometer (Varian, Cary Eclipse) and the images of 2,7–dichlorofluorescein (DCF) fluorescence were taken by using a fluorescence microscope (Carl Zeiss, Axiovert 40 CFL,USA).

Statistical Analysis

The effect of TBO and SeNP-TBO conjugate on *S. mutans* biofilm formation was compared with control biofilms (without any supplement) and analyzed using Student's t-test. Data with $P<0.05$ were considered statistically significant.

RESULTS

Characterization of Selenium Nanoparticle (SeNP)

Synthesis of Selenium nanoparticle was performed by reduction of Sodium Selenite by Ascorbic Acid. An orange colloidal solution of SeNP was formed. Synthesis of SeNP was monitored by UV-vis absorption spectroscopy. The UV spectrum of different concentrations of SeNP (Fig. 1) shown distinct peak at ~288 nm, which were confirmed the successful synthesis of SeNP in this study.

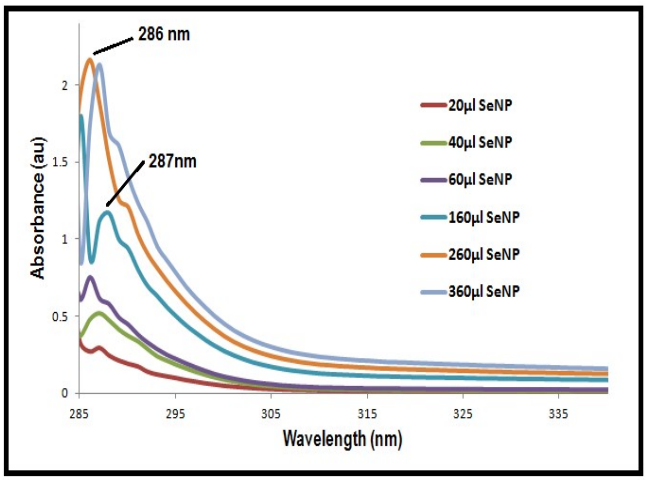

Fig. 1: UV-absorption spectra of SeNP at different concentration of SeNP

Size and shape of formed nanoparticles was assessed by transmission electron microscopy Fig. 2 (A) showed the TEM images of SeNP. The synthesized Selenium nanoparticles were uniform and spherical in shape with average size ~100 nm. In FTIR spectra of SeNP there were strong absorption band around 3425cm^{-1}, 2928 cm^{-1} and 1647 cm^{-1}. An FTIR spectrum of SeNP is shown in Fig. 2 (B).

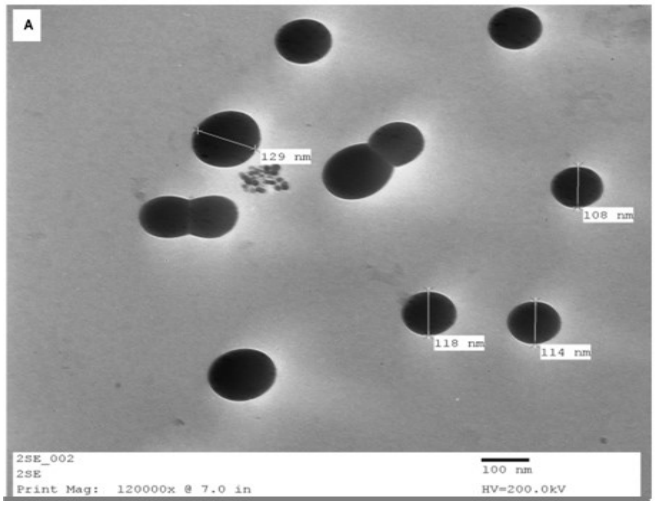

Fig. 2 (A) TEM micrograph of SeNP

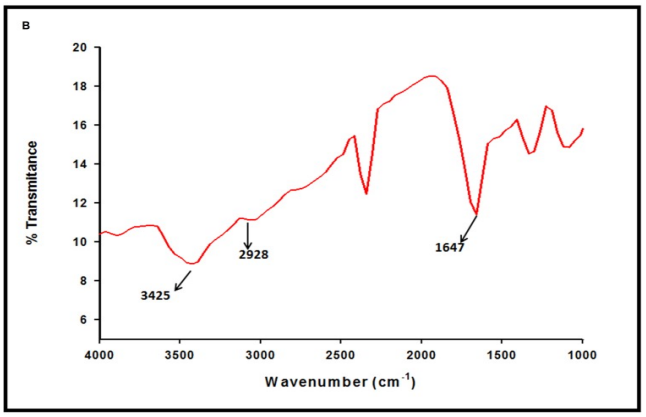

Fig. 2 (B) FTIR spectra of SeNP

Minimum Inhibitory Concentration (MIC) and Minimum Bactericidal Concentration (MBC)

SeNP showed no minimum inhibitory effect on *S. mutans* cells after serial dilution (initial concentration 1 mg/mL) on microtiter plate. TBO were showed MIC and MBC of 62. 5 µg/mL and 125 µg/mL respectively whereas in presence of SeNP showed MIC and MBC of 31.25 µg/mL and MBC of 62.5 µg/mL. SeNP–TBO conjugate showed two-fold higher activities against *S. mutans* than TBO alone.

Physicochemical Interaction of TBO with SeNP

The maximum absorption spectrum of SeNP measured by UV-visible spectroscopy was at 288 nm as shown in Fig. 3. TBO showed maximum absorption peaks at 675 and 585 nm. After gradual addition of SeNP concentrations in the presence of a constant concentration of TBO, there was no change in maximum absorption peaks. The UV-Vis absorption result suggests that there is no interaction between TBO and SeNP and TBO is not present on the surface of SeNP.

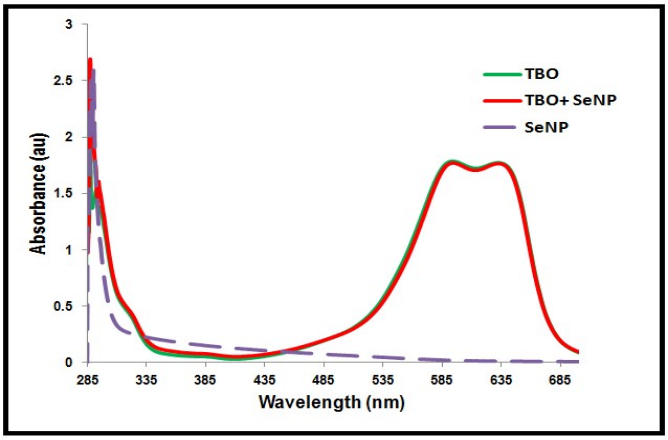

Fig. 3 UV-absorption spectra showing no interaction of SeNPs and TBO

Fluorescence spectroscopy was used to determine the enhancement or quenching of TBO after conjugation with SeNPs. In fluorescence emission spectra, there is enhancement of fluorescence of TBO fluorescence in the presence of nanoparticle (Fig. 4). This was shown that SeNP are enhancing the photodynamic therapy. It can be predicted from both the above experiments that TBO is not attached on the surface of SeNP but accompanying the SeNPs.

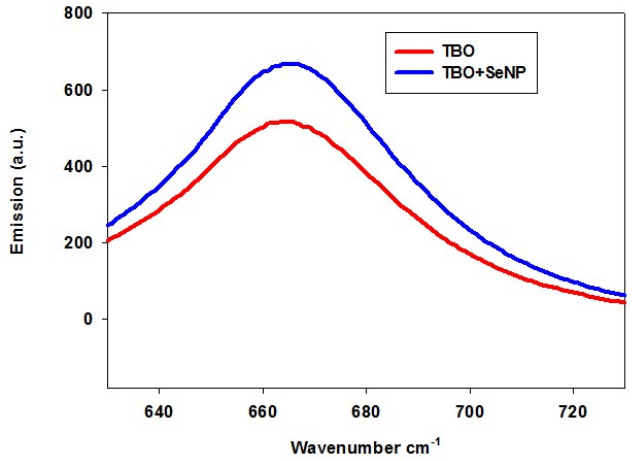

Fig. 4 Fluorescence emission spectra of TBO in absence and presence of SeNP

Quantitation of Biofilm Formation

The antibiofilm activities of TBO and SeNP–TBO were observed by using crystal violet and XTT biofilm reduction assays. Crystal violet assay has been used widely to measure biofilm formation because of its amenability to large screening procedures. Crystal violet dye was used to measure percent inhibition on biofilm formation in the presence of different compounds because it affects diffusion as well as morphological and physiological differences in individual cells that influence dye binding. A crystal violet assay revealed a maximum percent inhibition of *S. mutans* biofilm formation after 24 hours' incubation, recorded as 20% and 60% by TBO (31.25 µg/mL) and SeNP–TBO (31.25 µg/mL; TBO) conjugate, respectively (Fig. 5).

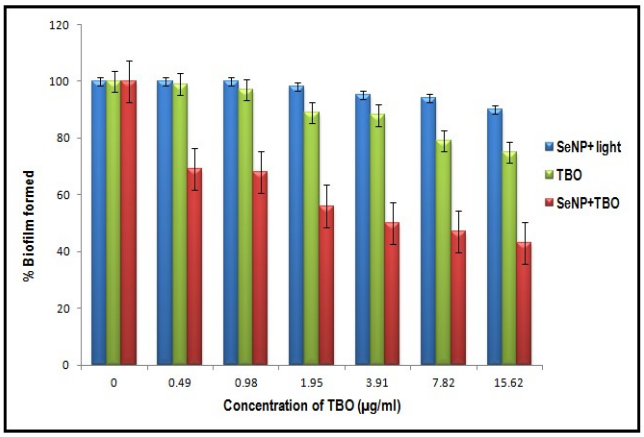

Fig. 5 Crystal violet biofilm reduction assay bar plot

XTT reduction assay was performed for quantitative measurement of *S. mutans* biofilm formation. This assay is the most commonly used test to estimate viable biofilm growth and examine the impact of biofilm therapies. There was almost 32% loss in viability in presence of SeNP-TBO conjugate whereas in presence of only TBO there was 22% loss is viability of cells. SeNP alone in presence of light showed almost negligible loss of viability (Fig. 6).

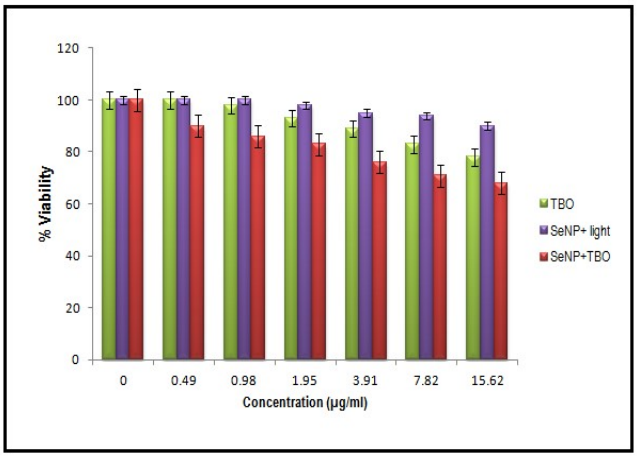

Fig. 6 XTT reduction assay bar plot representing % loss in viability

Fluorescence Microscopy Analysis of Reduction in Biofilm

The structure of the biofilm of *S. mutans* was examined under the Fluorescence scanning microscope to observe the changes shown in Fig. 7 A & B. In the absence of treatment (control), the cells showed clumping which was not seen in case of samples treated with sub inhibitory concentration. Unlike control, the cells in treated samples were clearly dispersed and no clump formation was observed.

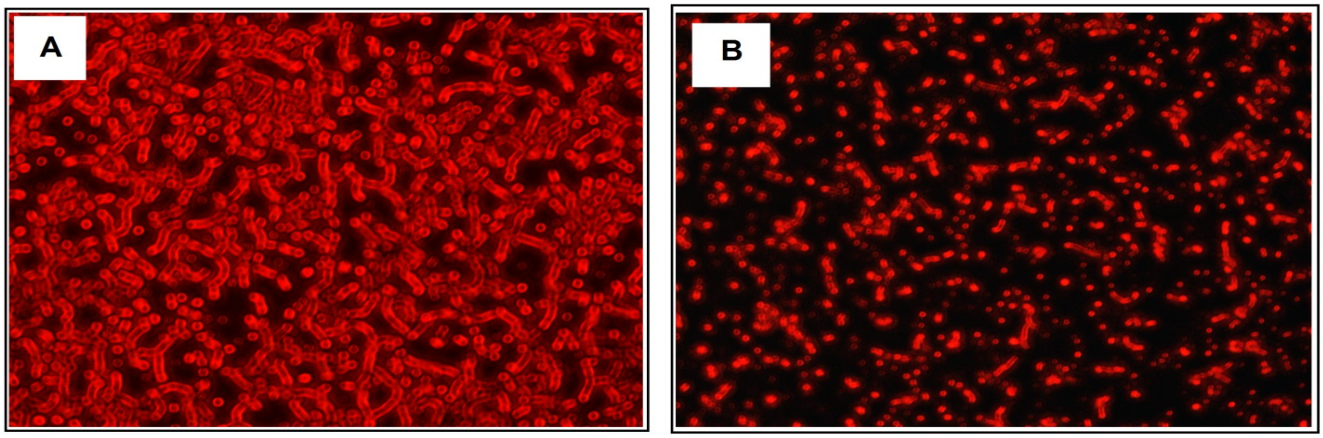

Fig. 7 (A) Control *S. mutans* biofilm (B) Treated *S. mutans* biofilm

Quantification of ROS formation

The formation of reactive oxygen species (ROS) has been suggested to be one of the fundamental mechanisms of SeNPs. In order to determine if the mechanism of killing by SeNP, TBO, and SeNP-TBO was ROS mediated, we used fluorescence based assay in combination with fluorescent spectroscopy, to monitor the generation of ROS in the *S. mutans* cells incubated at various time intervals. The cell permanent dye DCFH-DA is oxidized by peroxinitrite ($ONOO^-$) and hydroxyl radicals (OH°) to yield the fluorescent molecule 2,7-dichlorofluorescein. Generation of ROS by SeNP was monitored by incubation for 30 and 60 min time interval, which showed the significance of ROS generation as compared to control *S. mutans* biofilm (Fig. 8). Fluorescence, resulting from oxidation of dye DCFH-DA was observed indicating the presence of ROS.

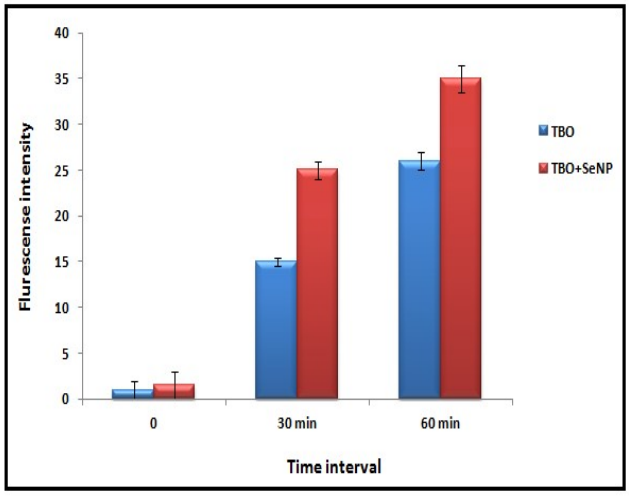

Fig. 8 Quantification of ROS (Fluorescence intensity) at various time intervals after treatment

DISCUSSION

The essential role of *Streptococcus mutans* in the pathogenesis of caries is well authenticated. It still continues to affect a large section of population. It establishes the infection by influencing various virulence traits like acidogenecity, synthesis of exopolysaccharides (glucan), aciduracity, hydrophobicity, cell to cell signaling (quorum sensing), adherence and biofilm formation.[28] Management of dental caries involves prescribing therapeutic regimens to individuals according to their risk levels and optimal conservative treatment decisions.[29] Based on this premise, different approaches to control cariogenic biofilms, including the use of antimicrobial agents, have been employed for dental disinfection.[30] But there is need to develop novel strategies in order to aim at the elimination of such cariogenic biofilms.

In the last two decades, nanobiotechnologists have gained more interest in inorganic nanoparticles, mostly metallic nanoparticles that are now used for bioconjugation and biological imaging in drug delivery and diagnostic applications. [31-32] Metallic nanoparticles have a large surface area, and this helps the interaction of a broad gamut of drug molecules. [33]

Nobel metallic nanoparticles such as colloidal SeNPs are attracting significant interest as carriers of various payloads towards the target. These payloads are antitumor agents and other drugs. [34-35] Metallic nanoparticles have some unique chemical and physical properties that make them efficient carriers and enhancers. GNP has remarkable surface plasmon resonance for imaging and fluorescence enhancing or quenching of attached drugs or dyes. [36-37] This is first study where Selenium nanoparticle are used to enhance photodynamic effect of TBO. The current study focuses on the use of PDT performed with TBO in presence of SeNP, since a better understanding of *S. mutans* photo inactivation is an important issue in Dentistry.

Synthesis of selenium nanoparticle was performed by reduction with Ascorbic acid. The change in color of solution to orange confirmed the formation of nanoparticle. Furthermore, characterization of SeNPs with various spectroscopic and microscopic studies bolstered the formation of selenium nanoparticle. TEM analysis revealed the formation of uniform spherical nanoballs of selenium. The absorption spectra of selenium nanoparticles have clear maximum around 280 nm. The nature of the spectra matches very well with those reported earlier.[38] The reported results indicate that Se sols, with particles of mean diameter 100 nm or more,

show an absorption peak at 300 nm or higher wavelength, depending on the size, while those with smaller particles do not show any regular absorption peak in the UV-visible region. Comparisons of the observed spectra with the reported ones indicate that the average particle diameter is about 100 nm or smaller.

FT-IR spectrum for pure L-ascorbic acid has been reported to show stretching vibration of the carbon-carbon double bond and the peak of enol hydroxyl at 1674 cm^{-1} and 1322 cm^{-1}, respectively.[39] These peaks disappeared after the reaction and new peaks were observed at 3425 cm^{-1}, 1647 cm^{-1}. These peaks correspond to the hydroxyl and conjugated carbonyl groups, respectively. These results indicate the presence of the polyhydroxyl structure on the surface of SeNP. The polyhydroxyl structure has an excellent dispersion effect on SeNPs.

Earlier studies have been performed against pathogenic microbes by amalgamating the properties of both colloidal GNP and thiazine dyes such as MB and TBO as a GNP–thiazine conjugate. In one of the studies, GNP conjugated with TBO showed effective PDT against *Staphylococcus aureus* and enhanced the bactericidal effect up to 90%–99%.[40] Recently, in another study, GNP-conjugated biodegradable and biocompatible poly(lactic-co-glycolic acid) PGLA with MB embedded showed effective antimicrobial PDT against *Enterococcus faecalis* infected tooth root canal.[40]

In this study selenium nanoparticle enhanced photodynamic activity of TBO. In presence of SeNP, TBO showed MIC of 32.25µg/mL against *S. mutans* which was much better than TBO alone (62.5 µg/mL).Enhanced PDT in presence of Gold nanoparticle has been accounted earlier but there are no reports on SeNP enhanced photodynamic therapy.

The spectroscopic techniques were used to determine the type of interaction between TBO and SeNP. UV absorption spectra of clearly showed no enhancement of peak of TBO in presence of SeNP which is indicative that TBO is not on surface of SeNP. It has been reported that there are four types of interaction between nanoparticle and photosystem (PS); PS embedded in NP, PS bound to surface of NP and PS alongside NP.[41] From fluorescence spectroscopy results it is confirmed that in presence of SeNP fluorescence of TBO is increasing that means SeNP is enhancing PDT of TBO by accompanying the PS.

Crystal violet assay showed a considerable reduction in biofilm there is almost 60% reduction in biofilm in SeNP-TBO combination while there is only 20% reduction in presence of TBO alone. XTT assay showed the viability of cells and there is 32% and 22% reduction in viability in presence of SeNP-TBO and TBO. This may be inferred from above discussion that SeNP is not killing the *S. mutans* that extent that it effect the normal flora of mouth but it is reducing the biofilm formation of *S. mutans*. Moreover morphological changes in biofilm structure can be clearly seen in fluorescence micrograph (Fig. 7).

Photosensitizers in PDT have been reported to kill bacteria by producing ROS (Reactive oxygen Species).[42] In our study ROS production was confirmed by conducting a fluorescence based assay in combination with fluorescence spectroscopy. The fluorescence resulting from oxidation of dye DCFH-DA was observed indicating the presence of ROS, which was much higher in case of SeNP in combination with TBO as compared to TBO alone. This justifies the enhanced antibiofilm activity of SeNP-TBO in comparison to TBO alone.

CONCLUSIONS

Our study evaluates the antibacterial and antibiofilm activity of Selenium nanoparticle enhanced photodynamic therapy with TBO as photo sensitizer. Spectroscopic and microscopic techniques along with biofilm reduction assay were used to justify the results. This is the first time we have developed an alternative, efficient, and novel SeNP-mediated *S. mutans* antibiofilm PDT approach. Microbial biofilm is one of the most important factors in the worldwide increase of multiple drug-resistant pathogens. Therefore, this novel approach may be a good alternative to control infection in hospital and clinical settings.

REFERENCES

[1] Costerton JW, Stewart PS, Greenberg EP. Bacterial biofilms: a common cause of persistent infection. Science. 1999; 284:1318-1322.

[2] Donlan RM. Biofilms: microbial life on surfaces. Emerg Infect Dis. 2002; 8:881–890.

[3] Costerton JW, Lewandowski Z, Caldwell DE, Korber DR, Lappin-Scott HM. Microbial biofilms. Annu Rev Microbiol. 1995; 49:711–745.

[4] Douglas LJ. Medical importance of biofilms in Candida infections. Rev Iberoam Micol. 2002; 19:139–143.

[5] Costerton, Lewandowski, Caldwell DE, Korber DR, Lappin-Scott HM. Microbial biofilms. Annu. Rev. Microbiol. 1995; 49:711-745.

[6] O'Toole GA, Gibbs KA, Hager PW, Phibbs PV, Kolter R. The global carbon metabolism regulator Crc is a component of a signal transduction pathway required for biofilm development by *Pseudomonas aeruginosa.* J. Bacteriol. 2000; 182:425-431.

[7] Miller MB, Bassler BL. Quorum sensing in bacteria. Annu. Rev. Microbiol. 2001; 55:165-199.

[8] Parsek A, MR, Greenberg EP. Acyl-homoserine lactone quorum sensing in gram-negative bacteria: a signaling mechanism involved in associations with higher organisms. Proc. Natl. Acad. Sci. USA. 2000; 97: 8789-8793.

[9] Kievit D, TR, Iglewski BH. Bacterial quorum sensing in pathogenic relationships. Journal of Infection and Immunity. 2000; 68:4839-4849.

[10] Xu KD, McFeters GA, Stewart PS. Bioflm resistance to antimicrobial agents. Microbiol. 2000; 146: 547-549.

[11] Aslam S. Effect of antibacterials on biofilms. Am J Infect Control. 2008; 236:S175.

[12] Hamada, Shigeyuki, Hutton D. Slade. Biology, Immunology and Cariogenicity of *S. mutans*. *Journal of* Microbiology Reviews. 1980; 44(2): 331-84.

[13] Wilson BC, Patterson SM. The physics, biophysics and technology of photodynamic therapy. Phy. Med. Biol. 2008; 53: 61–109.

[14] Kubler AC. Photodynamic therapy. Med. Laser Appl. 2005; 20:37–45.

[15] Ochsner M. Photophysical and photobiological processes in the photodynamic therapy of tumors. J. Photochem. Photobiol. B: Biol. 1997; 39:1–18.
[16] Cadet JJL, Ravanat GR, Martinez MH, Medeiros P, Di Mascio. Singlet oxygen oxidation of isolated and cellular DNA: product formation and mechanistic insights. Photochem. Photobiol. 2006; 82: 1219–1225.
[17] Schmidt R. Photosensitized generation of singlet oxygen. Photochem. Photobiol. 2006; 82: 1161–1177.
[18] Malik Z, Hanania J, Nitzan Y. Bactericidal effects of photoactivate porphyrins–an alternative approach to antimicrobial drugs. J. Photochem. Photobiol. 1990; B5 281–293.
[19] Bhatti M, Macrobert A, Meghji S, Henderson B, Wilson M. Effect of dosimetric and physiological factors on the lethal photosensitization of *Porphyromonas gingivalis* in vitro. Photochem. Photobiol. 1997; 65 1026–1031.
[20] Cheng Y, Samina AC, Meyers JD *et. al.* Highly efficient drug delivery for gold nanoparticle vectors for *in vivo* photodynamic therapy of cancer. J. Am. Chem. Soc. 2008; 130:10643-10647.
[21] Jain PK, Huang X, El-Sayed IH, El-Sayed MA. Review of some interesting surface plasmon resonance enhanced properties of noble metallic nanoparticles and their applications to biosystems. Plasmonics. 2007; 2:107-118.
[22] Qian Li, Tianfeng Chen, Fang Yang, et al. Facile and controllable one-step fabrication of selenium nanoparticles assisted by L-cysteine. Materials Letters, 2010, 64: 614–617.
[23] Tobudic S, Kratzer C, Lassnigg A, Graninger W, Prester E. *In vitro* activity of antifungal combinations against *Candida albicans* biofilms. *J* Antimicrob Chemother. 2010; 65:271–274.
[24] Djordjevic D, Wiedmann M, McLandsborough LA. Microtiter plate assay for assessment of *Listeria monocytogenes* biofilm formation. Appl Environ Microbiol. 2002; 68:2950–2958.
[25] Jin Y, Zhang T, Samaranayake YH, Fang HHP, Yip HK, Samaranayake LP. The use of new probes and stains for improved assessment of cell viability and extracellular polymeric substances in *Candida albicans* biofilms. Mycopathologia. 2005; 159:353–360.
[26] Bridier A, *et al.* Deciphering biofilm structure and reactivity by multiscale time-resolved fluorescence analysis. Adv. Exp. Med. Biol. 2011; 715:333–349.
[27] Zielonka J, Kalyanaraman B. ROS- generating mitochondrial DNA mutations can regulate tumor cell metastasis- A critical commentary. Free Radic Biol Med. 2008; 45:1217–1219.
[28] Hasan S, Danishuddin M, Adil M, Singh K , Verma PK, Khan AU. Efficacy of *E. Officinalis* on the cariogenic properties of *Streptococcus mutans*: a novel and alternative approach to suppress quorum-sensing mechanism. Plos one. 2012; 7:e40319.
[29] Anusavice K. Clinical decision-making for coronal caries management in the permanent dentition. J. Dent. Educ. 2001; 65:1143–1146.
[30] Wolff MS, Larson C. The cariogenic dental biofilm: good, bad or just something to control? Braz. Oral. Res. 2009; 23: 31–38.
[31] Daniel MC, Astruc D. Gold nanoparticles: assembly, aupramolecular chemistry, quantum-size-related properties, and applications toward biology, catalysis, and nanotechnology. Chem. Rev. 2004; 104:293–346.
[32] Parak WJ, Gerion D, Pellegrino T. Biological applications of colloidal nanocrystals. Nanotechnology, 2003; 14: R15–R27.
[33] Li J, Wang X, Wang C. The enhancement effect of gold nanoparticles in drug delivery and as biomarkers of drug-resistant cancer cells. Chem Med Chem. 2007; 2:374–378.
[34] Han G, Ghosh P, Rotello VM. Functionalized gold nanoparticles for drug delivery. Nanomedicine. 2007; 2:113–123.
[35] Tam F, Goodrich GP, Johnson BR, Halas NJ. Plasmonic enhancement of molecular fluorescence. Nano. Lett. 2007; 7:496–501.
[36] Glomm WR. Functionalized gold nanoparticles for applications in bionanotechnology. *J.* Dispers. Sci. Technol. 2005; 26:389–414.
[37] Shah CP, Kumar M, Pushpa KK, Bajaj PN. Acryl onitrile-induced synthesis of polyvinyl alcohol-stabilized selenium nanoparticles. Crystal Growth & Design, 2008; 8(11):4159-4164.
[38] Xiong J, Wang Y, Xue Q, Wu X. Synthesis of highly stable dispersions of nanosized copper particles using L-ascorbic acid. Gree. Chem. 2011; 13: 900.
[39] Narband N, Tubby S, Parkin IP. Gold nanoparticles enhance the toluidine blue-induced lethal photosensitisation of *Staphylococcus aureus*. Curr Nanosci. 2008; 4:409–414.
[40] Pagonis TC, Chen J, Fontana CR. Nanoparticle-based endodontic antimicrobial photodynamic therapy. J Endod. 2010; 36:322–328.
[41] Perni S, Prokopovich P, Pratten J, Parkin IP,Wilson M. Nanoparticles: Their potential use in antimicrobial photodynamic therapy. Photochem. Photobiol. Sci. 2010; 10:712-720.
[42] Williams GJ, Pearson MJ, Wilson CM. The effect of variable energy input from a novel light source on the photo-activated bactericidal action of toluidine blue O on *Streptococcus mutans*, Caries Res. 2003; 37:190–193.

How to cite this article:
Haris Z, Khan AU: Selenium Nanoparticle Enhanced Photodynamic Therapy against Biofilm forming *Streptococcus mutans*. *Int. J. Life. Sci. Scienti. Res.,* 2017; 3(5):1287-1294. DOI:10.21276/ijlssr.2017.3.5.4
Source of Financial Support: Nil, **Conflict of interest:** Nil